The effect of AGN feedback on Sunyaev-Zel'dovich properties of simulated galaxy clusters

Dunja Fabjan[1,2], Susana Planelles[3,4], Stefano Borgani[2,4,5], Giuseppe Murante[2], Elena Rasia[2,12], Veronica Biffi[2,4], Nhut Truong[6], Cinthia Ragone-Figueroa[2,9], Gian Luigi Granato[2], Klaus Dolag[7,8], Elena Pierpaoli[10], Alexander M. Beck[7], Lisa K. Steinborn[7], Massimo Gaspari[11]

[1] Faculty of Mathematics and Physics, University of Ljubljana, Slovenija; [2] INAF – Astronomical observatory of Trieste, Italy; [3] Departamento de Astronomía y Astrofísica, Universidad de Valencia, Spain; [4] Astronomy Unit, Department of Physics, University of Trieste, Italy; [5] INFN – National Institute for Nuclear Physics, Italy; [6] Dipartimento di Fisica, Università di Roma Tor Vergata, Italy; [7] University Observatory Munich, Germany; [8] Max-Planck-Institut für Astrophysik, Munich, Germany; [9] Instituto de Astronomía Teórica y Experimental (IATE), Consejo Nacional de Investigaciones Científicas y Técnicas de la República Argentina (CONICET), Observatorio Astronómico, Universidad Nacional de Córdoba, Argentina; [10] University of Southern California, Los Angeles, USA; [11] Department of Astrophysical Sciences, Princeton University, Princeton, USA; Einstein and Spitzer Fellow; [12] Department of Physics, University of Michigan, USA

Abstract

The accurate measure of the masses of galaxy clusters is one of the most important goals in order to use them as tracers of cosmic evolution. To calibrate cluster total mass a number of observable quantities can be used. However, physical processes in galaxy clusters (e.g. AGN feedback) can affect the observed properties of the IntraCluster Medium (ICM), having a non negligible impact on the determined masses.

We studied the imprints that feedback from Active Galactic Nuclei leaves on the intracluster plasma during the assembly history of galaxy clusters, focusing on the pressure profiles and on the ICM properties observed via Sunyaev-Zel'dovich (SZ) effect.

To this purpose we used state-of-the-art cosmological hydrodynamical simulations based on an updated version of the TreePM–SPH GADGET-3 code. We present data from an extended set of galaxy clusters (around 100 clusters with masses above $3\cdot10^{13}$ M⊙/h) simulated with different prescriptions for the physics of baryons.

Simulations

NR – non-radiative hydrodynamical simulations based on the improved SPH formulation presented in *Beck et al. (2016)*

CSF – simulations accounting for the effects of radiative cooling, star formation, supernovae (SN) feedback and metal enrichment. Stellar evolution and metal enrichment are based on the model by *Tornatore et al. (2007)*. Metal-dependent radiative cooling rates and the effects of a uniform UV/X-ray background radiation are included accordingly to models by *Wiersma et al. (2009)* and *Haardt & Madau (2001)*. Kinetic feedback from galactic outflows powered by SN explosions is based on *Springel & Hernquist (2003)* and is characterized by a wind velocity of *350 km/s*.

AGN – includes same physical processes as in the CSF case plus the effect of AGN feedback.

The subgrid model for super-massive black hole (SMBH) accretion and AGN feedback has been presented in *Steinborn et al. 2015*:

• mechanical outflows and radiation are combined and included in form of *thermal feedback*: $\dot{E}=(\epsilon_0+\epsilon_f\,\epsilon_r)\,\dot{M}_\bullet c^2$

where for the outflow and radiative efficiency, ϵ_0 and ϵ_r, variable values are computed depending on the BH mass and on accretion rate, while the fraction of the radiative feedback coupled to the surrounding gas as thermal feedback is fixed at $\epsilon_f = 0.05$

• the efficiency of radiative and mechanical feedback depend on both the (Eddington-limited) gas accretion rate and the SMBH mass, providing a smooth transition between radio and quasar mode: $\dot{M}_\bullet=min(\dot{M}_{B,hot}+\dot{M}_{B,cold},\dot{M}_{Edd})$

Eddington-limited gas accretion onto BHs is computed by multiplying the Bondi rate by a boost factor α; in this work we neglect hot gas accretion (α_{hot} = 0) and consider only cold gas accretion, for which the Bondi accretion rate is boosted by a factor α_{hot} = 100

Cluster dynamical state

From the parent DarkMatter simulation (1 Gpc/h comoving size, 1024^3 particles) 29 Lagrangian regions were extracted and resimulated. The "complete sample" is composed by the whole cluster population of ~100 clusters with $M_{500} > 3\cdot10^{13}$ M⊙/h, whereas the "reduced sample" is made by the 29 massive central clusters and groups.

Clusters in the AGN simulation were further classified in:

• **regular/disturbed** according to their global dynamical state, with two methods: a) the centre shift, defined as the offset between the position of the cluster minimum gravitational potential and its center of mass in units of its virial radius, b) the mass fraction contributed by substructures

• **CC**(cool-core)**/NCC**(non-cool-core)-like halos according to their core thermodynamical properties; the former have low central gas entropy and metal-enriched gas, while the latter are objects with isentropic gas cores with no evidence of a central peaked metallicity;

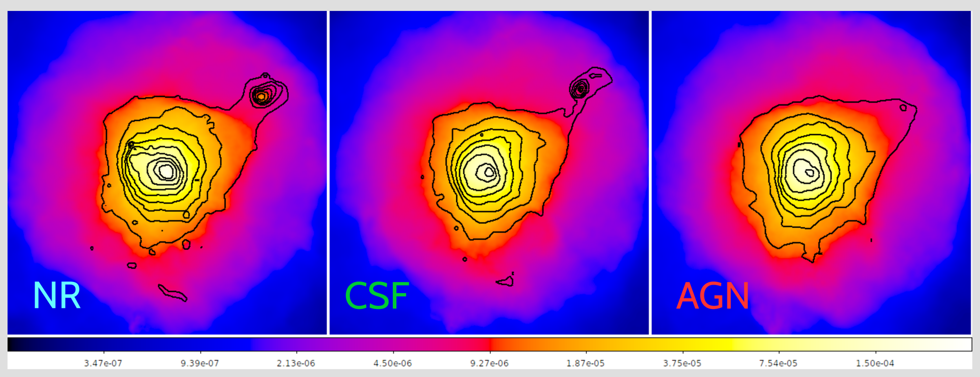

Maps of the projected Compton-y signal with superimposed X-ray surface brightness contours (black) for a massive cluster at z = 0 classified as relaxed and CC (above) and unrelaxed and NCC (below). Maps have a side length of 4.4 R_{500}. The color code for y is equal in both panels and displayed below them. Contours from X-ray surface brightness maps obtained using bolometric cooling function are plotted in 9 logarithmically equispaced levels in the range 10^{-8} to 10^{-3} erg cm^{-2}.

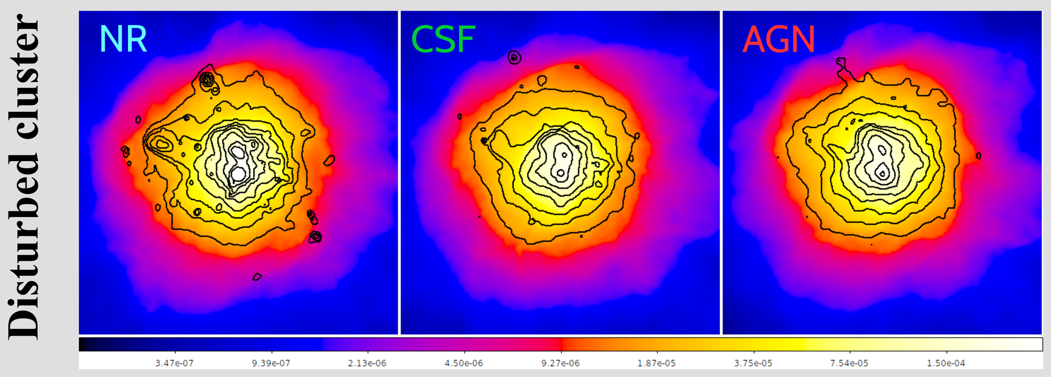

Pressure profiles and cool-coreness

The pressure profile of the intracluster gas is computed by assuming an ideal gas equation of state. To compare them with observations the simulated profiles are scaled with P_{500} (*see equation below*).

$$P_{500} = 1.45 \times 10^{-11}\,\mathrm{erg\,cm^{-3}}\left(\frac{M_{500}}{10^{15}\,h^{-1}M_\odot}\right)^{2/3} E(z)^{8/3}$$

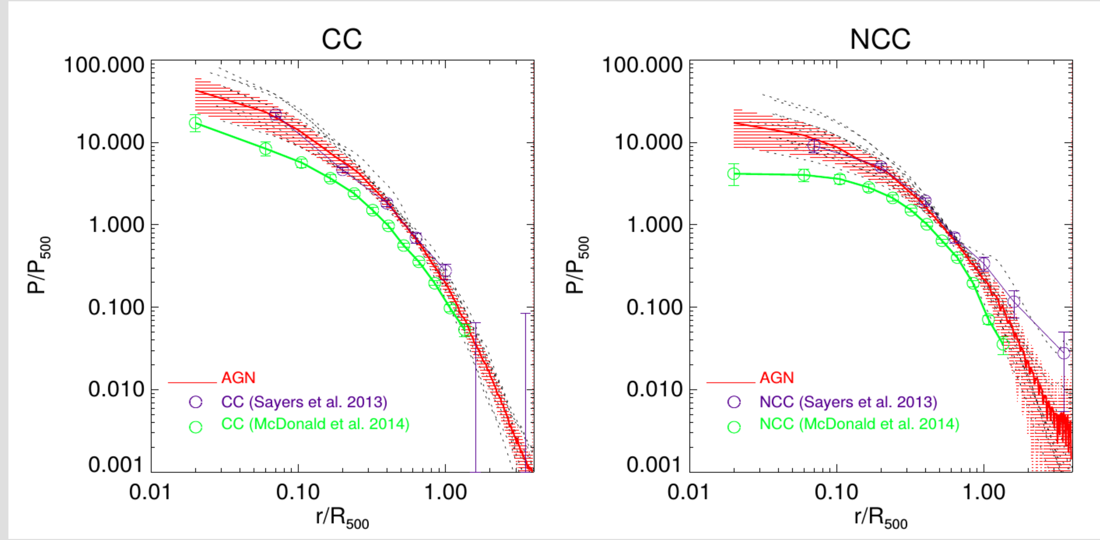

Mean radial profiles of scaled pressure, P/P_{500}, out to 4·R_{500} at z = 0 for CC (left panel) and NCC (right panel) clusters within our AGN simulations. Individual profiles are shown with thin dotted black lines. The mean profile of each sample is represented by a continuous red line surrounded by a shaded area representing 1-σ scatter around the mean profile. Comparison is made with average pressure profiles of observed CC and NCC clusters from Sayers et al. (2013) (purple open circles with error bars) and McDonald et al. (2014) (green open circles with error bars).

◆ mean profiles of CC/NCC clusters are in good agreement with each other at intermediate radii ($0.2<r/R_{500}<1$) and as expected clearly diverge from each other in inner cluster regions ($r/R_{500}\leq0.2$)

◆ in general, both cluster populations show a consistency within 1-σ with the observations by *Sayers et al. (2013)*, especially in inner cluster regions; mean pressure profile of NCC systems is lower in cluster outskirts ($r>R_{500}$), being in better agreement with the observational determinations by *Arnaud et al. (2010)* or *Planck Collaboration et al. (2013d)*

◆ mean profile of NCC objects has a higher dispersion, especially in the outer regions, than for the sample of CC clusters; the larger dispersion in cluster outskirts is mostly produced by a clumpier gas distribution in outer regions of disturbed massive galaxy clusters

Y_{SZ}–M and Y_{SZ}-Y_X scaling relations

The SZ effect is proportional to the integrated thermal pressure of the intracluster medium along the line of sight and therefore it is an ideal proxy for the gas mass (and cluster total mass). The Y_X parameter, the X-ray equivalent in the integrated SZ effect, is defined as the product of the gas mass with the cluster temperature.

◆ Y_{SZ}-M and Y_{SZ}-Y_X relations (*right panels*) are close to self-similar for simulated clusters, with a scatter of 0.06-0.07 and 0.03-0.04 respectively

◆ at the scale of massive clusters scaling relations for different simulations agree with observational data; in addition, consistently with previous numerical analysis, results at R_{500} for the complete sample do not show any significant dependence on the included physics

◆ small changes in the pressure profiles depending on either the dynamical state or the cool-coreness of the considered systems have a different impact on the corresponding Y_{SZ}−M relation (*see table*); therefore, cluster dynamical state measured at R_{500} is not strongly correlated with its cool-coreness

Simulation	Sample	A_{500}	B_{500}	$\sigma_{log_{10}Y_{500}}$
NR	Complete	-4.282 ± 0.008	1.688 ± 0.012	0.062
CSF	Complete	-4.382 ± 0.008	1.726 ± 0.011	0.062
AGN	Complete	-4.305 ± 0.009	1.685 ± 0.013	0.067
	Reduced-CC	-4.253 ± 0.028	1.561 ± 0.071	0.047
	Reduced-NCC	-4.291 ± 0.015	1.618 ± 0.037	0.055
	Reduced-Regular	-4.316 ± 0.013	1.639 ± 0.025	0.032
	Reduced-Disturbed	-4.249 ± 0.038	1.518 ± 0.105	0.073

Best-fit parameters for the normalization, A_{500}, the slope, B_{500}, and the scatter, $\sigma_{log10(Y500)}$, describing the relation between Y_{SZ} and cluster mass evaluated within R_{500}. The pivot X_0 is equal to $5\cdot10^{14}$ M⊙. The parameters are obtained for the complete sample of clusters and groups within the NR, CSF and AGN simulations. We also show the best-fit parameters obtained for the subsamples of regular/disturbed and CC/NCC systems in the AGN case.

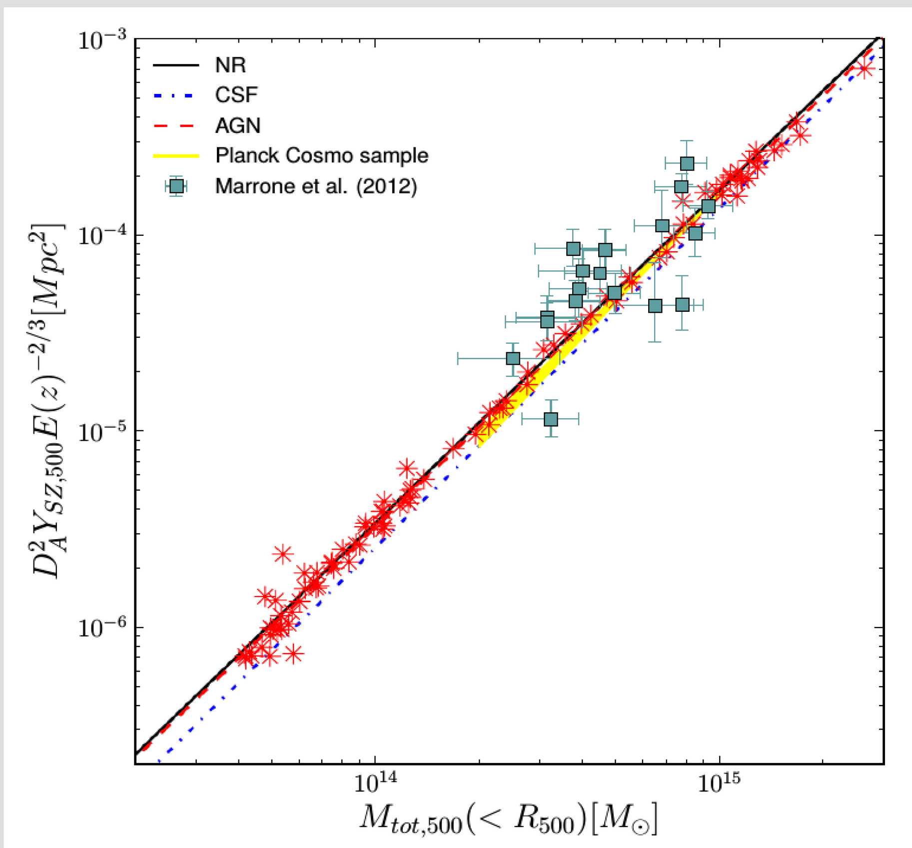

Relation between cylindrically integrated SZE flux and cluster mass within R_{500} for the sample of simulated clusters. We plot the best-fit relation obtained for the NR (black continuous line), CSF (blue dot-dashed line) and AGN (red dashed line) simulations, while only data for the AGN run are plotted (red asterisks). Observational samples used for comparison: data from Marrone et al. (2012) LoCuSS-SZA clusters are shown as light-blue squares with error bars, while the best-fit relation obtained for the Planck Cosmo sample is shown with the yellow shaded area (Planck Collaboration et al. 2014).

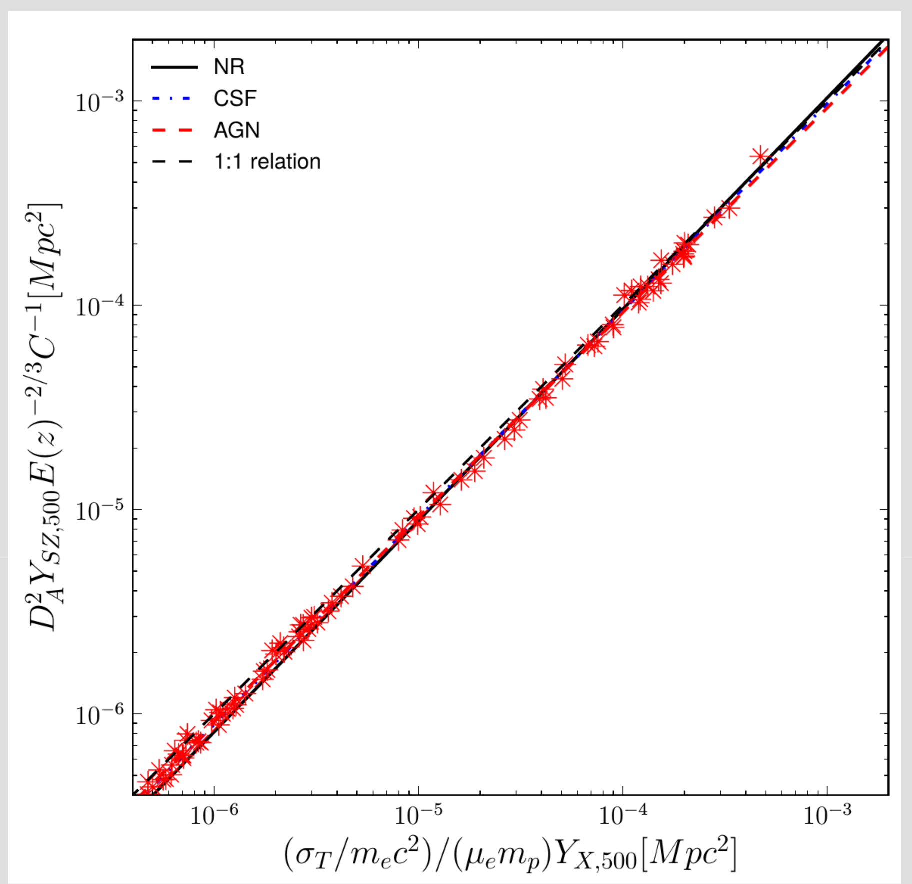

Relation between the cylindrically integrated SZE flux and Y_X at R_{500} for the complete sample of simulated systems. Best-fit relations are plotted with black continuous, blue dash-dotted and red dashed line for the NR, CSF and AGN simulations. For the sake of clarity, data (red asterisks) are plotted only for the AGN case. Y_X is evaluated using core-excised (0.15–1R_{500}) spectroscopic–like temperatures. The black dashed line stands for the identity relation.

Y_{SZ}–M evolution with redshift

◆ in all our models we found that the normalization and slope of the scaling relation do not show redshift evolution but only an increase in scatter; if we focus only on massive clusters, scatter remains constantly at low levels of about 0.03-0.05

◆ the residual variation of cluster properties in radiative simulations with respect to non-radiative ones is a consequence of overcooling that removes gas from the hot phase; including AGN feedback partially prevents cooling and brings NR and AGN normalization to be closer

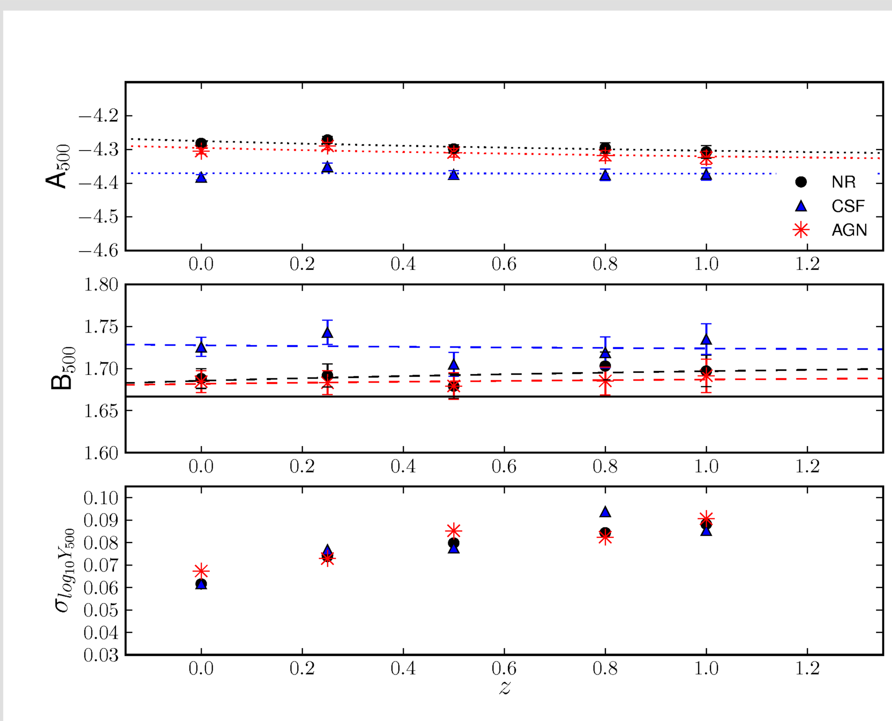

Redshift evolution of the $Y_{SZ,500}$–M_{500} scaling relation for the complete set of groups and clusters in the NR (black circles), AGN (red asterisks) and CSF (blue triangles) cases. In the three panels (from top down) we show the evolution of the normalization A_{500}, the slope B_{500}, and the scatter, $\sigma_{log10(Y500)}$, of the relation. For the normalization and the slope we overplot, with dotted and dashed lines respectively, the best-fit relation for redshift evolution. The self-similar value for the slope is represented in the middle panel with a black continuous line.

References

Planelles, S., Fabjan, D., et al. 2016, to appear in MNRAS
Steinborn, L. K., Dolag, K., Hirschmann, M., Prieto, M. A., & Remus, R.-S. 2015, MNRAS, 448, 1504
Rasia, E., Borgani, S., Murante, G., et al. 2015, ApJL, 813, L17
Truong, N., Rasia, E., Mazzotta, P., et al. 2016, arXiv:1607.00019
Biffi, V., Borgani, S., Murante, G., et al. 2016, ApJ, 827, 112

Further information: dunja.fabjan@fmf.uni-lj.si